SCIENCE CHINA
Life Sciences

•RESEARCH PAPER•

February 2020 Vol.63 No.2: 251–258
https://doi.org/10.1007/s11427-018-9405-y

The bacterial RNA ligase RtcB accelerates the repair process of fragmented rRNA upon releasing the antibiotic stress

Muhammad Ramzan Manwar[1,2†], Changjun Shao[1†], Xing Shi[1,2†], Jian Wang[1], Qiang Lin[1], Yigang Tong[3], Yu Kang[1*] & Jun Yu[1,2*]

[1]*CAS Key Laboratory of Genome Sciences and Information, Beijing Institute of Genomics, Chinese Academy of Sciences, Beijing 100101, China;*
[2]*University of Chinese Academy of Sciences, Beijing 100190, China;*
[3]*Beijing Institute of Microbiology and Epidemiology, Beijing 100071, China*

Received August 20, 2018; accepted October 10, 2018; published online June 26, 2019

RtcB, a highly conserved RNA ligase, is found in all three domains of life, and demonstrated to be an essential tRNA splicing component in archaea and metazoans. However, the biological functions of RtcB in bacteria, where there is no splicing, remains to be clarified. We first performed bioinformatics analysis which revealed highly conserved structures and presumably conserved functions of RtcB in bacteria. However, its orthologs only occur in ~0.5% of bacterial species across diverse phyla with significant signals of frequent horizontal transfer, highlighting its non-essential role in bacteria. Next, by constructing an *rtcB*-knockout strain, we find that the removal of antibiotic stress induces a significant impact on *rtcB* expression in wild-type strain, and furthermore the depletion of RtcB (ΔRtcB strain) delays the recovery process. Our transcriptomic analysis, comprising the 3′-end labeling of RNAs, highlights a significant increase in unmapped reads and cleaved rRNAs in the ΔRtcB strain, particularly during recovery. Our observations suggest that the conserved RNA ligase RtcB, repairs damaged rRNAs following stress, which potentially saves energy and accelerates recovery of its host. We propose that acquisition of RtcB by diverse bacterial taxa provides a competitive advantage under stressful conditions.

RtcB, bacteria, RNA ligase, stress response, ribosomal RNA, RNA repair

Citation: Manwar, M.R., Shao, C., Shi, X., Wang, J., Lin, Q., Tong, Y., Kang, Y., and Yu, J. (2020). The bacterial RNA ligase RtcB accelerates the repair process of fragmented rRNA upon releasing the antibiotic stress. Sci China Life Sci 63, 251–258. https://doi.org/10.1007/s11427-018-9405-y

INTRODUCTION

RtcB is a widely conserved RNA ligase found in a wide range of eubacterial, archaeal, and eukaryotic taxa but is non-universal (Burroughs and Aravind, 2016). The ligation function of RtcB was first proposed when its crystal structure was solved in the archaeon *Pyrococcus horikoshii* (Okada et al., 2006). As a ligase, RtcB contains key amino acid residues involved in binding two Mn^{2+} and four sulfate (SO_4^{2-}) ions together with GMP (Englert et al., 2012; Maughan and Shuman, 2016; Okada et al., 2006). Later studies not only revealed details of the binuclear Mn^{2+} active center, the guanylylated-histidine, and reactive RNA ends binding to the sulfate ions in the vicinity (Desai et al., 2014a; Englert et al., 2012), but also provided thorough characterization of Mn^{2+}/GTP dependence and guanylylation during ligation (Desai et al., 2013; Nandy et al., 2017). Experiments conducted *in vitro* have demonstrated that RtcB directly joins the RNA strands ending with a 2′,3′-cyclic phosphate or 3′-phosphate to the 5′-hydroxyl group of another RNA end in a GTP/Mn^{2+}-

†Contributed equally to this work
*Corresponding authors (Yu Kang, email: kangy@big.ac.cn; Jun Yu, email: junyu@big.ac.cn)

dependent manner (Tanaka et al., 2011a). The detailed ligation mechanism can perfectly repair damaged RNAs and does not introduce any addition or deletion (Chakravarty and Shuman, 2012; Chakravarty et al., 2012). Furthermore, RtcB was also characterized with its *in vitro* "sealing and healing" function for fragmented DNA (Das et al., 2013; Das et al., 2014).

RtcB has rather limited sequence homology with other classical RNA ligases in fungi and plants, thereby its encoding gene is proposed as the long-sought RNA ligase in animals (Englert et al., 2011), where *rtcB* often appears together with *archease* (Desai et al., 2015; Desai et al., 2014b; Popow et al., 2014). As the 3′-phosphate and 5′-OH ends of RNA are often generated by RNases damage and cannot be repaired by canonical RNA ligases, RtcB has been proposed to play key roles in RNA repair and the underlying stress-protection mechanisms (Burroughs and Aravind, 2016; Tanaka and Shuman, 2011). Furthermore, *rtcB* orthologs are experimentally validated as essential components of tRNA splicing and maturation in archaea (Englert et al., 2011) and metazoans (Popow et al., 2011; Tanaka et al., 2011b). In addition, RtcB was shown to be involved in the cytoplasmic mRNA splicing of *X-box binding protein 1* (*XBP1*) which initiates the unfolded protein response (UPR) in metazoans (Kosmaczewski et al., 2014; Lu et al., 2014), and neuroprotection (Kosmaczewski et al., 2015; Ray et al., 2014; Song et al., 2015) and antibody secretion (Jurkin et al., 2014). However, the presence of the *rtcB* homolog in bacteria and its orthologs among bacterial species still remains a mystery in terms of physiological function, other than RNA splicing. A recent report has revealed a significant role of RtcB in repairing broken rRNA ends produced by the site-specific ribotoxin, MazF, in *E. coli* (Temmel et al., 2016), and another study has highlighted its role in rRNA homeostasis during stress of ribosome-targeting antibiotics (Engl et al., 2016). Both studies demonstrate RtcB as part of a previously unrecognized adaptive response linking ribosome homeostasis with basic cell physiology and behaviour. However, some questions still remain: (ⅰ) what is the prevalence and predicted function of *rtcB* gene in various bacterial taxa? (ⅱ) Does RtcB protect the host from stress induced by antibiotics-other than ribotoxins, particularly the most widely used antibiotics that target cell wells? (ⅲ) Does the ligation activity of RtcB occur in a site-specific manner, such as the MazF cleavage site, or more generally to all broken sites produced under specific physiological conditions, for which direct evidence from transcriptome analysis is still lacking?

Here, we first delineate the prevalence and functional conservation of *rtcB* orthologs in bacterial taxa, using updated databases, and then report functional studies starting with the construction of *rtcB*-knockout mutants in *E. coli*. In transcriptome analysis with labeled 3′-termini of RNAs, RtcB exhibits a significant role in rRNAs repair and accelerates recovery after release from the stress of cell-wall-targeting antibiotics.

RESULTS AND DISCUSSION

The *rtcB* gene has conserved ligase function but is not essential in bacterial taxa

We first curated the UniProt Database where *rtcB* was found widely distributed in the three domains of life (Popow et al., 2011). In Eubacteria, all the sequences of *rtcB* homologs possess conserved motifs involved in the ligation mechanism via metal and GTP binding sites (Figure S1 in Supporting Information), and the predicted 3D structure of the *E. coli* RtcB protein has strong similarity to its homologs in human and archaea (Figure S2 in Supporting Information), suggesting that its function is conserved in eubacteria. However, such apparent functional conservation is not supported by its distribution in bacteria. Orthologs of *rtcB* are present in all major lineages, but only in approximately 0.5% of bacterial species and 5% of archaeal species curated so far in the database (Figure 1A). Within bacterial lineages, the presence of *rtcB* varies from phylum to phylum, where Elusimicrobia carries the highest percentage at 15.4%, and Terrabacteria occupies the lowest at 0.4%. In Proteobacteria, the largest bacterial phylum, the *rtcB* prevalence was observed with ~0.5% of sequenced genomes (Figure 1A), where δ-Proteobacteria appeared to have the highest prevalence (1.6%) (Figure 1B). Of note, *rtcB* is not present in all strains of *E. coli*, and not in the core genome-organizational-framework (GOF) (Kang et al., 2014) of the species. We also checked the essentiality of *rtcB* using the OGEE database (Chen et al., 2017), and found that the non-essentiality of *rtcB* is also supported by experiments in *E. coli* and *Salmonella enterica*. Therefore, *rtcB* is widely distributed but not highly prevalent across bacterial lineages, and such features suggest possible non-essential physiological functions which are perhaps advantageous under specific environmental conditions.

We further investigated the phylogeny of *rtcB* orthologs among bacterial phyla (Figure S3 in Supporting Information), which highlights the horizontal acquisition of *rtcB* orthologs across distant lineages, such as the species pair of *Legionella messillensis* and *L. hackeliae* (Figure S3 in Supporting Information). I further support, a previous report has found that *rtcB* was carried and transferred through an IS element together with other accessory genes in species of *Salmonella enterica* (Ygberg et al., 2006). The syntenic order of *rtcB* and its neighboring genes illustrates the non-conserved genetic structure across phyla and even within Proteobacteria lineages (Figure S4 in Supporting Information). However, the well investigated *rtcBA* operon and transcriptional regulator, *rtcR*, in *E. coli*, were found as an

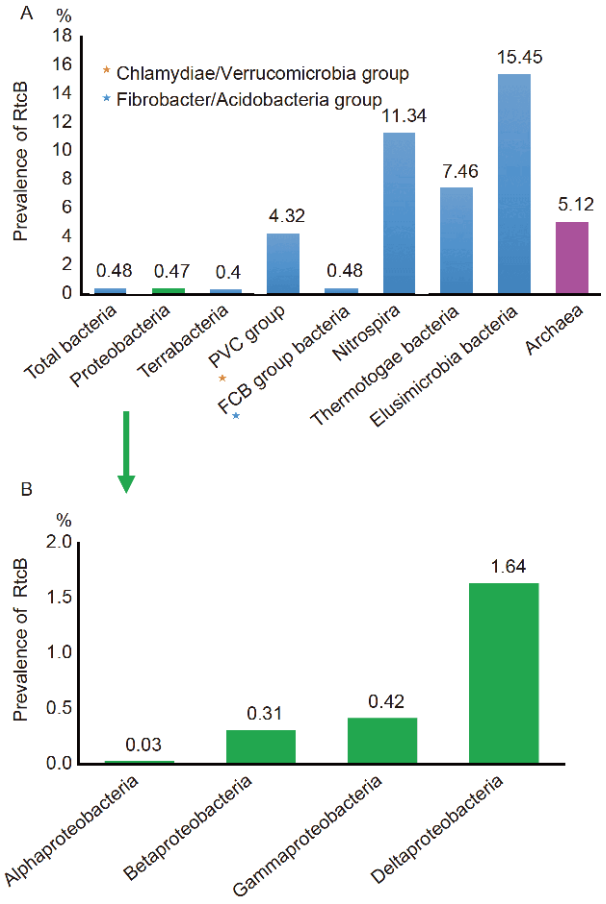

Figure 1 Distribution of *rtcB* in bacteria. A, Percentage prevalence of *rtcB* in all major phyla; B, in each Proteobacteria class.

exception in gamma-Proteobacteria species. All these evidences suggest that the *rtcB* is highly prone to transfer between bacterial taxa, whether closely or distantly related.

RtcB accelerates recovery by repairing broken RNAs

We constructed an *rtcB*-knockout *E. coli* strain for investigating its *in vivo* functions under antibiotic-induced stress. In normal culture and the culture with the cell-wall targeting antibiotic ceftriaxone, the *rtcB* wild-type strain only showed marginal, if any, protective effects (Figure S5 in Supporting Information), as proposed in a previously reported ribotoxins-induced stress environment (Engl et al., 2016; Temmel et al., 2016). However, the wild-type strain shows the higher rate of stress recovery, as compared to the knockout strain, upon removal of ceftriaxone (Figure S5 in Supporting Information). This behavior is similar to that observed following stress release in MazF—the site specific rRNA cleaver (Temmel et al., 2016).

The mRNA expression of *rtcB* shows remarkable up-regulation upon release from the ceftriaxone stress, relative to the undetectable level under the normal condition and during ceftriaxone treatment (Figure S6 in Supporting Information). From *in situ* hybridization (ISH) analysis, employing a fluorescence-labeled probe hybridized with the *rtcB* mRNA, we find that only a small proportion of cells express *rtcB*, although the number and level of *rtcB* expressing cells increases upon removing ceftriaxone (Figure S6 in Supporting Information), suggesting the positive effects of *rtcB* on stress recovery.

The RNA-Seq results of 3′-end-sequencing show that only a small portion (0.06%–0.1%) of reads carry the 3′-end labeling, and almost none is labeled at the 3′-end of mature 16S rRNA suggesting that the 3′-end of mature 16S rRNA is difficult to label possibly due to some physiological termini protective mechanisms (Figure 2). When we normalize the count of labeled reads at each site in rRNA by the coverage of the same sites, we find two major peaks for all samples, in both strains, for each time point during the stress and recovery. One is labeled to the premature 16S rRNA with an extra 33 nt at the 3′-end, and the other is the mature 3′-end of 23S rRNA. Except for the two peaks, other labeled reads are sparsely distributed along the rRNA gene, showing no hotspot of RNA cleavage. Comparing with the ΔRtcB strain, the wild strain shows a much higher level of both peaks at each time point, and an apparent decrease is observed when stress is released (Figure 2). However, the same trend is not observed in the ΔRtcB strain which highlights the ligation effects of RtcB in wild type strain.

For the majority of the unlabeled reads, over 90% are mapped to the rRNAs for each sample. However, compared to the wild strain, the ΔRtcB strain contains 38% more unmapped reads (4.0% vs. 2.9%) which include single reads that are not mapped to the *E. coli* genome and paired-end reads mapped in opposite direction, with insert size >1 kb. For both strains, 55%–60% of the unmapped reads are junction reads mapped to two sites of the genome. The junction sites (supported by at least two split reads) are widely dispersed across the whole genome without any sign of hotspots (Figure 3A), but the number of junctions correlates well to read coverage (or expression level) in each 100-bp genomic window (Figure 3B). This indicates that the junction reads are randomly generated by template switching during reverse-transcription or PCR amplification, and not ligated by RtcB. In qRT-PCR analysis, upon normalizing to internal control of complete 16S rRNA, we find much higher abundance of RNAs carrying three representative junction sites in the ΔRtcB mutant, compared to the wild-type strain, at each time-point during the process of stress and recovery. Our result suggests more complete 16S rRNA in wild type as read coverages of all the representative junctions are similar for both strains (Figure 3C).

In antibiotic-induced stress environments, other than ribotoxins, the rRNA can also be fragmented by the release of endogenous RNases normally stored in the periplasm which can be triggered by various of lethal toxins especially those

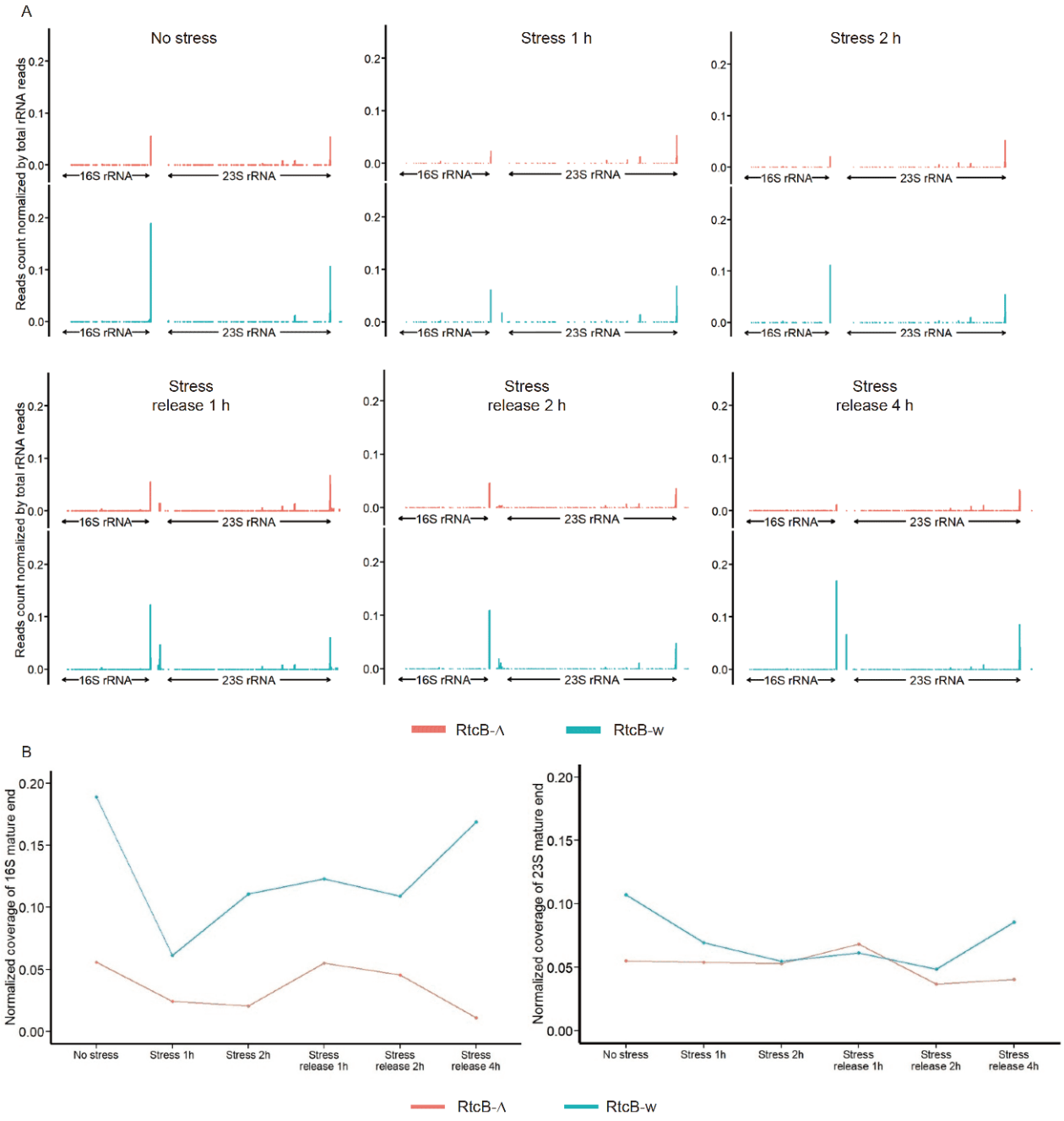

Figure 2 The natural 3′-end sequencing results. A, The natural 3′-end sequencing results for RtcB-Δ and RtcB-w samples at time points of no stress, ceftriaxone stress for one hour, two hours, stress released for one hour, two hours, and four hours. The *x*-axis indicates the sequence of 16S and 23S genes in the rRNA operon, and the *y*-axis indicates the count of labeled reads normalized by coverage of the same site. Graphs of strain RtcB-Δ (upper) and RtcB-w (lower) are showcased in pair for each time points. B, The normalized reads of mature ends of 16S (left) and 23S (right). In RtcB-Δ strain, the mature ends of 16S and 23S are lower than those in RtcB-w strain, and the mature ends of 16S and 23S in RtcB-w could recover after antibiotic release while they could not recover after antibiotic release in RtcB-Δ.

that attack the cell wall. Upon stress removal, surviving cells have two ways to deal with the damaged rRNAs: one way leads to the degradation of damaged rRNAs by RNA exonuclease such as the very efficient polynucleotide phosphorylase (PNPase), followed by re-synthesis of new rRNA for re-growth, which are obviously energy-consuming (Burroughs and Aravind, 2016; Kaczanowska and Rydén-Aulin, 2007). The second route comprises the repair of broken RNAs with RNA ligase, such as RtcB, to restore the translational activity of ribosomes, and thus saves energy and supports fast recovery from stress. Since rRNA comprises over 90% of total RNAs, biogenesis of a small portion of ribosome will consume considerable amount of cell energy, and makes the host cells less fit under competitive circum-

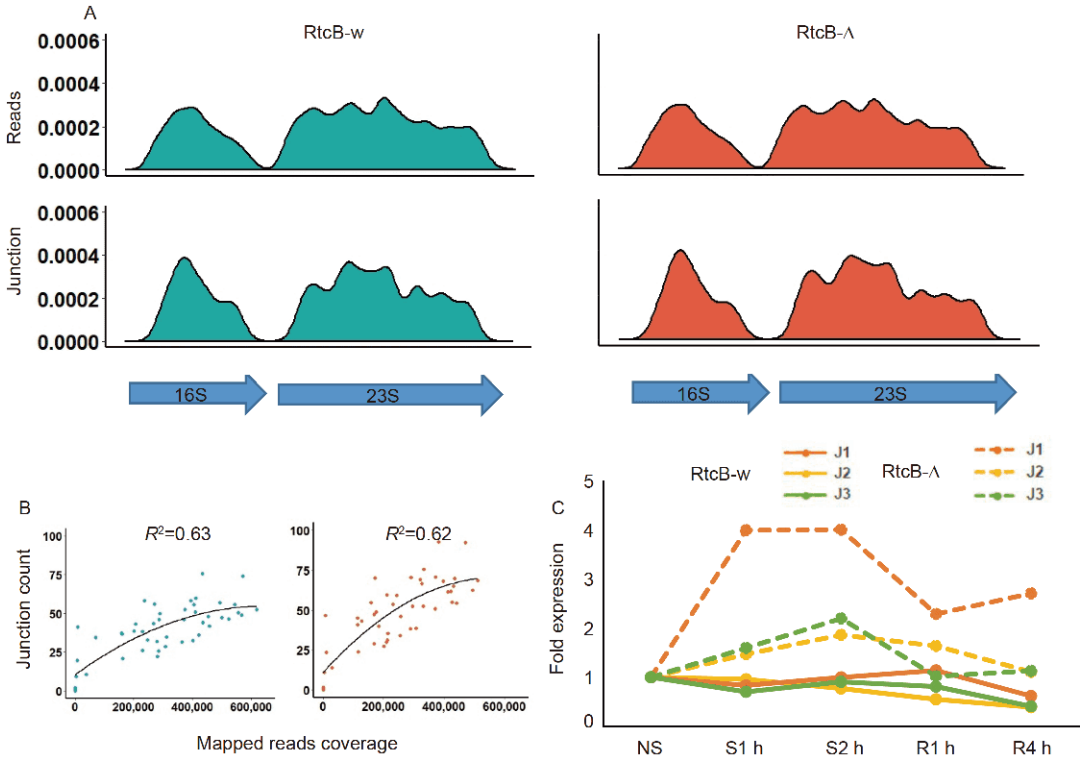

Figure 3 RtcB ligates broken rRNA to restore ribosome activity. A, The upper panel indicates the density distribution of read coverage along 16S rRNA and 23S rRNA, and the lower panel illustrates the density distribution of junction sites along 16S rRNA and 23S rRNA. The values of *y*-axis show the density estimation of reads or junctions. B, The positive relationship of read coverage and junction count in the same window of rRNA. C, Detection of three representative junctions in serial time points by qRT-PCR. NS, no stress; S1 and S2, stress for 1 and 2 h; R1h and R4h, stress released for 1 and 4 h.

stances. Our transcriptome results show that the RtcB only repairs the damaged RNAs, especially rRNA, and does not introduce false ligations of random free ends. The perfect repair by RtcB is impressive, and is possibly enabled by the physical interaction between RtcB and ribosome. A previous study has shown that RtcB proteins interact with ribosomes and can be co-eluted (Temmel et al., 2016). Such a distribution suggests that rRNAs, when cleaved by RNA endonuclease at some sites, possibly remain in place due to the structural integrity of ribosomal proteins, and the interacting RtcB can subsequently ligate the broken ends. As RtcB only interacts with ribosomes that keep their structural integrity, it will not ligate free rRNAs released from ribosomes that have collapsed, which would instead be degraded by RNA exonuclease in the cell.

Our results do not show obvious sign of site-specificity for RtcB ligation. First, the split reads and free 3′ ends are randomly distributed along rRNA, and we could not find characteristic motifs around the junction sites or free ends for both strains, which indicates random cleavage by RNases. Second, the free 3′ ends within rRNA of wild-type strain are clearly decreased relative to those of the RtcB-knockout strain. Therefore we propose that the repair of broken rRNA by RtcB is not site-specific but depends on the RNA fragments being held in place by a structurally intact ribosome. Thus RtcB can be seen to provide a surveillance function to screen post-stress ribosomes for cleaved rRNA fragments and to repair them by ligation.

MATERIALS AND METHODS

Evolutionary conservation analysis

Protein sequences of RtcB homologs of all species are retrieved from the most updated UniProt database, and aligned with Clustal Omega (http://www.ebi.ac.uk/Tools/msa/clustalo/) (Li et al., 2015; McWilliam et al., 2013). A phylogenetic tree was construct by using Mega7 software (http://megasoftware.net/) (Kumar et al., 2016), and neighboring genes synteny of *rtcB* were assessed using SyntTax (http://archaea.u-psud.fr/SyntTax/) (Oberto, 2013). The full length protein models of RtcB in *E. coli* were generated using the I-TASSER platform (http://zhanglab.ccmb.med.umich.edu/I-TASSER/) (Roy et al., 2010; Yang et al., 2015), and visualized with UCSF-Chimera (http://www.cgl.ucsf.edu/chimera) (Huang et al., 2014; Pettersen et al., 2004).

Strains and materials

An in-house conserved *E. coli* MG1655 strain was used as

the wild type control strain, and the *rtcB* gene was knocked out by inserting a chloramphenicol-resistant gene with the Lambda red system (pKD46, λ-red), as previously described (Juhas and Ajioka, 2016). The knockout strain was verified with Sanger sequencing of the recombinant site and exhibited phenotypic change of increased motility (Engl et al., 2016). Both strains were cultured in LB medium at 37°C unless specified. Ceftriaxone was added at 1 μg mL^{-1} in a survival assay (Liu et al., 2011).

Real-time quantitative PCR

Total RNA was extracted using TRIzol reagent (Invitrogen, USA), and treated with DNase I. Reverse transcription was performed using SuperScript III Reverse Transcriptase. The RT-qPCR was performed by using Real-Time qPCR System (Applied Biosystems) and SYBR Green PCR Master Mix (Applied Biosystems), according to the manufacturer's instruction. Relative concentrations of targeting RNAs were normalized to full length 16S rRNA. Primers for 16S, *rtcB* and three junction sites are 16S-F: CGGACGGGTGAGTAATGTCT, 16S-R: CTCAGACCAGCTAGGGATCG; *rtcB*-F: CTCAACGCTCACCACTTCTG, *rtcB*-R: CAGCGTTCCCAGGTGTTTAT; Junction 1-F: TGGGAACTGCATGACGCT, Junction 1-R: TTAACCTTGCGGCCGTACT; Junction 2-F: ACTGCCTGATAGAGGGGGGT, Junction 2-R: CCTCCAAGTCGACATCGTTT; and Junction 3-F: TGAGTCTCGTGGAGGGGGAT, Junction 3-R: TAATCCCATCTGGGCACATC.

Super resolution imaging for ISH of *rtcB* in *E. coli*

We fixed the *E. coli* cells in 4% formaldehyde solution by following the manufacturer's instructions and labeled the *rtcB* mRNA with probes designed by ThermoFisher, then followed the *in situ* hybridization (ISH) cell assay procedure for suspension cells (QuantiGene ViewRNA ISH). Labeled cells were imaged using activator-emitter dye pairs (Alexa 680 and Alexa 750 as emitters) through the platform of SRiS-NBI (STROM) imaging.

Natural 3′-end labeling RNA-Seq and transcriptome analysis

RNA samples were extracted at serial time points during the ceftriaxone stress and removal of ceftriaxone for both ΔRtcB and wild-type strains without removing rRNAs. Single-stranded pre-adenlyated DNA adapters (5′rApp-GATCGGAAGAGCACACGTCT NH_2-3′) were ligated to the pre-dephosphorylated 3′-ends of sample RNA by a truncated T4 RNA Ligase 2 (NEB #K227Q) at 25°C and then reverse transcribed with both N6 random primer and specific primer to adaptor by SuperScript II Reverse Transcriptase. The cDNA products were subjected to RNA-Seq procedure following the Illumina Hiseq2000 strand-specific kit instruction and sequenced as pair-end reads of 100 bp and achieve average 1.16 Gb raw reads per sample. After quality trimming, clear reads containing the 3′-end label were picked out. The *E. coli* str. K-12 substr. MG1655 genome sequence (NC_000913.3) downloaded from NCBI was used as a reference, and the ribosomal RNA operons except *rrnC* were masked by bedtools (v2.24.0). All qualified sequences after trimming were pooled together as single end reads, and mapped to reference by bowtie2 (v4.1.2). The number of labeling reads at each site is normalized to the coverage at the same site. Unmapped reads were aligned to reference by STAR (v2.5.1) to detect split reads.

Availability of data

The clear sequence data reported in this paper have been deposited in the Genome Sequence Archive (Wang et al., 2017) in BIG Data Center (Big Data Center Members, 2017), Beijing Institute of Genomics (BIG), Chinese Academy of Sciences, under accession numbers CRA000773, that are publicly accessible at http://bigd.big.ac.cn/gsa.

Compliance and ethics *The author(s) declare that they have no conflict of interest.*

Acknowledgements *This work was supported by the National Key Research and Development Program of China (2016YFC0903800), the National Scientific Foundation of China (31470180, 31471237, 31671350), the Programs of Beijing Municipal Science and Technology Project (Z171100001317011), the Scientific Research Project of Public Welfare Industry (2013FY114300, 201402018), the Key Research Program of Frontier Sciences, the Chinese Academy of Sciences (QYZDY-SSW-SMC017), and the CAS-TWAS President's Fellowship.*

References

Big Data Center Members, B (2017). The BIG Data Center: from deposition to integration to translation. Nucl Acids Res 45, D18–D24.
Burroughs, A.M., and Aravind, L. (2016). RNA damage in biological conflicts and the diversity of responding RNA repair systems. Nucl Acids Res 44, 8525–8555.
Chakravarty, A.K., and Shuman, S. (2012). The sequential 2′,3′-cyclic phosphodiesterase and 3′-phosphate/5′-OH ligation steps of the RtcB RNA splicing pathway are GTP-dependent. Nucl Acids Res 40, 8558–8567.
Chakravarty, A.K., Subbotin, R., Chait, B.T., and Shuman, S. (2012). RNA ligase RtcB splices 3′-phosphate and 5′-OH ends via covalent RtcB-(histidinyl)-GMP and polynucleotide-(3′)pp(5′)G intermediates. Proc Natl Acad Sci USA 109, 6072–6077.
Chen, W.H., Lu, G., Chen, X., Zhao, X.M., and Bork, P. (2017). OGEE v2: an update of the online gene essentiality database with special focus on differentially essential genes in human cancer cell lines. Nucl Acids Res 45, D940–D944.
Das, U., Chakravarty, A.K., Remus, B.S., and Shuman, S. (2013). Rewriting the rules for end joining via enzymatic splicing of DNA 3′-PO4 and 5′-OH ends. Proc Natl Acad Sci USA 110, 20437–20442.
Das, U., Chauleau, M., Ordonez, H., and Shuman, S. (2014). Impact of

DNA3′pp5′G capping on repair reactions at DNA 3′ ends. Proc Natl Acad Sci USA 111, 11317–11322.
Desai, K.K., Bingman, C.A., Phillips Jr., G.N., and Raines, R.T. (2013). Structures of the noncanonical RNA ligase RtcB reveal the mechanism of histidine guanylylation. Biochemistry 52, 2518–2525.
Desai, K.K., Bingman, C.A., Cheng, C.L., Phillips Jr., G.N., and Raines, R. T. (2014a). Structure of RNA 3′-phosphate cyclase bound to substrate RNA. RNA 20, 1560–1566.
Desai, K.K., Cheng, C.L., Bingman, C.A., Phillips Jr, G.N., and Raines, R. T. (2014b). A tRNA splicing operon: archease endows RtcB with dual GTP/ATP cofactor specificity and accelerates RNA ligation. Nucl Acids Res 42, 3931–3942.
Desai, K.K., Beltrame, A.L., and Raines, R.T. (2015). Coevolution of RtcB and archease created a multiple-turnover RNA ligase. RNA 21, 1866–1872.
Engl, C., Schaefer, J., Kotta-Loizou, I., and Buck, M. (2016). Cellular and molecular phenotypes depending upon the RNA repair system RtcAB of *Escherichia coli*. Nucl Acids Res 5, gkw628.
Englert, M., Sheppard, K., Aslanian, A., Yates, J.R., and Söll, D. (2011). Archaeal 3′-phosphate RNA splicing ligase characterization identifies the missing component in tRNA maturation. Proc Natl Acad Sci USA 108, 1290–1295.
Englert, M., Xia, S., Okada, C., Nakamura, A., Tanavde, V., Yao, M., Eom, S.H., Konigsberg, W.H., Söll, D., and Wang, J. (2012). Structural and mechanistic insights into guanylylation of RNA-splicing ligase RtcB joining RNA between 3′-terminal phosphate and 5′-OH. Proc Natl Acad Sci USA 109, 15235–15240.
Huang, C.C., Meng, E.C., Morris, J.H., Pettersen, E.F., and Ferrin, T.E. (2014). Enhancing UCSF chimera through web services. Nucl Acids Res 42, W478–W484.
Juhas, M., and Ajioka, J.W. (2016). Lambda red recombinase-mediated integration of the high molecular weight DNA into the *Escherichia coli* chromosome. Microb Cell Fact 15, 172.
Jurkin, J., Henkel, T., Nielsen, A.F., Minnich, M., Popow, J., Kaufmann, T., Heindl, K., Hoffmann, T., Busslinger, M., and Martinez, J. (2014). The mammalian tRNA ligase complex mediates splicing of *XBP1* mRNA and controls antibody secretion in plasma cells. EMBO J 33, 2922–2936.
Kaczanowska, M., and Rydén-Aulin, M. (2007). Ribosome biogenesis and the translation process in *Escherichia coli*. Microbiol Mol Biol Rev 71, 477–494.
Kang, Y., Gu, C., Yuan, L., Wang, Y., Zhu, Y., Li, X., Luo, Q., Xiao, J., Jiang, D., Qian, M., et al. (2014). Flexibility and symmetry of prokaryotic genome rearrangement reveal lineage-associated core-gene-defined genome organizational frameworks. mBio 5, e01867.
Kosmaczewski, S.G., Edwards, T.J., Han, S.M., Eckwahl, M.J., Meyer, B. I., Peach, S., Hesselberth, J.R., Wolin, S.L., and Hammarlund, M. (2014). The RtcB RNA ligase is an essential component of the metazoan unfolded protein response. EMBO Rep 15, 1278–1285.
Kosmaczewski, S.G., Han, S.M., Han, B., Irving Meyer, B., Baig, H.S., Athar, W., Lin-Moore, A.T., Koelle, M.R., and Hammarlund, M. (2015). RNA ligation in neurons by RtcB inhibits axon regeneration. Proc Natl Acad Sci USA 112, 8451–8456.
Kumar, S., Stecher, G., and Tamura, K. (2016). MEGA7: molecular evolutionary genetics analysis version 7.0 for bigger datasets. Mol Biol Evol 33, 1870–1874.
Li, W., Cowley, A., Uludag, M., Gur, T., McWilliam, H., Squizzato, S., Park, Y.M., Buso, N., and Lopez, R. (2015). The EMBL-EBI bioinformatics web and programmatic tools framework. Nucl Acids Res 43, W580–W584.
Liu, Y.Q., Li, J.R., Du, J.F., Hu, M., Bai, H., Qi, J., Gao, C., Wei, T.T., Su, H., Jin, J.L., et al. (2011). Accurate assessment of antibiotic susceptibility and screening resistant strains of a bacterial population by linear gradient plate. Sci China Life Sci 54, 953–960.
Lu, Y., Liang, F.X., and Wang, X. (2014). A synthetic biology approach identifies the mammalian UPR RNA ligase RtcB. Mol Cell 55, 758–770.
Maughan, W.P., and Shuman, S. (2016). Distinct contributions of enzymic functional groups to the 2′,3′-cyclic phosphodiesterase, 3′-phosphate guanylylation, and 3′-ppG/5′-OH ligation steps of the *Escherichia coli* RtcB nucleic acid splicing pathway. J Bacteriol 198, 1294–1304.
McWilliam, H., Li, W., Uludag, M., Squizzato, S., Park, Y.M., Buso, N., Cowley, A.P., and Lopez, R. (2013). Analysis tool web services from the EMBL-EBI. Nucl Acids Res 41, W597–W600.
Nandy, A., Saenz-Méndez, P., Gorman, A.M., Samali, A., and Eriksson, L. A. (2017). Homology model of the human tRNA splicing ligase RtcB. Proteins 85, 1983–1993.
Oberto, J. (2013). SyntTax: a web server linking synteny to prokaryotic taxonomy. BMC Bioinf 14, 4.
Okada, C., Maegawa, Y., Yao, M., and Tanaka, I. (2006). Crystal structure of an RtcB homolog protein (PH1602-extein protein) from *Pyrococcus horikoshii* reveals a novel fold. Proteins 63, 1119–1122.
Pettersen, E.F., Goddard, T.D., Huang, C.C., Couch, G.S., Greenblatt, D. M., Meng, E.C., and Ferrin, T.E. (2004). UCSF Chimera—a visualization system for exploratory research and analysis. J Comput Chem 25, 1605–1612.
Popow, J., Englert, M., Weitzer, S., Schleiffer, A., Mierzwa, B., Mechtler, K., Trowitzsch, S., Will, C.L., Lührmann, R., Söll, D., et al. (2011). HSPC117 is the essential subunit of a human tRNA splicing ligase complex. Science 331, 760–764.
Popow, J., Jurkin, J., Schleiffer, A., and Martinez, J. (2014). Analysis of orthologous groups reveals archease and DDX1 as tRNA splicing factors. Nature 511, 104–107.
Ray, A., Zhang, S., Rentas, C., Caldwell, K.A., and Caldwell, G.A. (2014). RTCB-1 mediates neuroprotection via XBP-1 mRNA splicing in the unfolded protein response pathway. J Neurosci 34, 16076–16085.
Roy, A., Kucukural, A., and Zhang, Y. (2010). I-TASSER: a unified platform for automated protein structure and function prediction. Nat Protoc 5, 725–738.
Song, Y., Sretavan, D., Salegio, E.A., Berg, J., Huang, X., Cheng, T., Xiong, X., Meltzer, S., Han, C., Nguyen, T.T., et al. (2015). Regulation of axon regeneration by the RNA repair and splicing pathway. Nat Neurosci 18, 817–825.
Tanaka, N., Chakravarty, A.K., Maughan, B., and Shuman, S. (2011a). Novel mechanism of RNA repair by RtcB via sequential 2′,3′-cyclic phosphodiesterase and 3′-phosphate/5′-hydroxyl ligation reactions. J Biol Chem 286, 43134–43143.
Tanaka, N., Meineke, B., and Shuman, S. (2011b). RtcB, a novel RNA ligase, can catalyze tRNA splicing and *HAC1* mRNA splicing *in vivo*. J Biol Chem 286, 30253–30257.
Tanaka, N., and Shuman, S. (2011). RtcB is the RNA ligase component of an *Escherichia coli* RNA repair operon. J Biol Chem 286, 7727–7731.
Temmel, H., Müller, C., Sauert, M., Vesper, O., Reiss, A., Popow, J., Martinez, J., and Moll, I. (2016). The RNA ligase RtcB reverses MazF-induced ribosome heterogeneity in *Escherichia coli*. Nucl Acids Res 1, gkw1018.
Yang, J., Yan, R., Roy, A., Xu, D., Poisson, J., and Zhang, Y. (2015). The I-TASSER suite: protein structure and function prediction. Nat Methods 12, 7–8.
Ygberg, S.E., Clements, M.O., Rytkönen, A., Thompson, A., Holden, D.W., Hinton, J.C.D., and Rhen, M. (2006). Polynucleotide phosphorylase negatively controls spv virulence gene expression in *Salmonella enterica*. Infection Immun 74, 1243–1254.
Wang, Y., Song, F., Zhu, J., Zhang, S., Yang, Y., Chen, T., Tang, B., Dong, L., Ding, N., Zhang, Q., et al. (2017). GSA: genome sequence archive. Genom Proteom Bioinf 15, 14–18.

SUPPORTING INFORMATION

Figure S1 Structure conservation of RtcB in bacteria. 3D structure similarity of bacterial RtcB protein to homologs in archaea and eukarya. The upper penal shows the protein structure of RtcB in three dimensional structural models of RtcB in (I) bacteria (*E. coli*), (II) eukarya (*H. sapiens*), and (III) archaea (*P. horikoshii*), the lower penal is the enlarged view of histidine residues orientation.

Figure S2 Conserved domains and functional amino acids of RtcB in various bacterial species compared to archaea and eukaryotes. Active or catalytic site (histidine) is highlighted in red color, metal binding residues in pink color and GTP-binding residues in green color. Asterisk (*) indicates the highly conserved residues, and colon (:) symbol highlights the conservation of properties between residues.

Figure S3 Phylogeny of *rtcB* in major clades of bacteria. This phylogeny tree shows the wide distribution of *rtcB* across the bacterial kingdom. The different species within the same clade are highlighted with the same color.

Figure S4 Synteny of the *rtcB* neighboring genes among major clades of Proteobacteria. The synteny of *rtcB* neighboring genes in *E. coli* is compared with genomes of other clades. The pink color arrows highlight the similar cyclase (*rtcA*) gene in different genomes and blue-grey color indicates *rtcR*. The genes that are not syntenic between *E. coli* and other selected genomes are indicated with white arrows.

Figure S5 RtcB confers rapid recovery from antibiotic stress in *E. coli*. The upper panel is the growth curve of wild-type strain and RtcB-Δ strain, and lower panel is the expression of *rtcB* gene at the same time points during antibiotic stress and recovery.

Figure S6 Spatial barcoding analysis *rtcB* mRNA. Upon releasing stress, the intensity and PhotoCount in wild-type strain significantly increases compared to 0 and 1-h stress, which significantly correlates with qPCR.

The supporting information is available online at http://life.scichina.com and https://link.springer.com. The supporting materials are published as submitted, without typesetting or editing. The responsibility for scientific accuracy and content remains entirely with the authors.